

EVIDENCE OF MULTIPLE SLOW ACOUSTIC OSCILLATIONS IN THE STELLAR FLARING LOOPS OF PROXIMA CENTAURI

A. K. SRIVASTAVA¹, S. LALITHA², AND J. C. PANDEY¹

¹ Aryabhata Research Institute of Observational Sciences (ARIES), Manora Peak, Nainital-263 002, India

² Hamburger Sternwarte, University of Hamburg, Gojenbergsweg 112, D-21029 Hamburg, Germany

Received 2013 August 19; accepted 2013 October 24; published 2013 November 12

ABSTRACT

We present the first observational evidence of multiple slow acoustic oscillations in the post-flaring loops of the corona of Proxima Centauri using *XMM-Newton* observations. We find the signature of periodic oscillations localized in the decay phase of the flare in its soft (0.3–10.0 keV) X-ray emissions. Using the standard wavelet tool, we find multiple periodicities of 1261 s and 687 s. These bursty oscillations persist for durations of 90 minutes and 50 minutes, respectively, for more than three cycles. The intensity oscillations with a period of 1261 s may be the signature of the fundamental mode of slow magnetoacoustic waves with a phase speed of 119 km s^{-1} in a loop of length $7.5 \times 10^9 \text{ cm}$, which is initially heated, producing the flare peak temperature of 33 MK and later cooled down in the decay phase and maintained at an average temperature of 7.2 MK. The other period of 687 s may be associated with the first overtone of slow magnetoacoustic oscillations in the flaring loop. The fundamental mode oscillations show dissipation with a damping time of 47 minutes. The period ratio P_1/P_2 is found to be 1.83, indicating that such oscillations are most likely excited in longitudinal density stratified stellar loops. We estimate the density scale height of the stellar loop system as $\sim 23 \text{ Mm}$, which is smaller than the hydrostatic scale height of the hot loop system, and implies the existence of non-equilibrium conditions.

Key words: magnetohydrodynamics (MHD) – stars: coronae – stars: flare – stars: individual (Proxima Centauri) – stars: oscillations (including pulsations) – waves

Online-only material: color figures

1. INTRODUCTION

The detection of magnetohydrodynamic (MHD) waves and oscillations may be very important in diagnosing the local plasma conditions of the coronae of the Sun and Sun-like stars by implying the principle of MHD seismology (e.g., Nakariakov & Verwichte 2005; Andries et al. 2009). MHD waves (e.g., Alfvén, slow, and fast magnetoacoustic waves) have been thoroughly explored and studied in the solar atmosphere (i.e., in its chromosphere and corona) using high resolution observations from the *Solar and Heliospheric Observatory (SOHO)*, *Transition Region and Coronal Explorer (TRACE)*, *Hinode*, *STEREO*, and the *Solar Dynamics Observatory (SDO)*, along with advances in theoretical modeling and simulations (e.g., Aschwanden et al. 1999; Nakariakov et al. 1999; Ofman & Wang 2002; O’Shea et al. 2007; Cirtain et al. 2007; De Pontieu et al. 2007; Verwichte et al. 2009; Jess et al. 2009; Srivastava & Dwivedi 2010; Aschwanden & Schrijver 2011; McIntosh et al. 2011; Kim et al. 2012; Mathioudakis et al. 2013, and references cited therein). These waves can transport the Sun’s photospheric powers into its chromosphere and corona in order to fulfill the fraction of energy losses. Advanced MHD seismology techniques have been developed to examine the crucial plasma conditions of the solar atmosphere based on the detection of multiple harmonics of MHD waves (e.g., McEwan et al. 2006, 2008; Verth & Erdélyi 2008; Srivastava et al. 2008; Andries et al. 2009; Wang 2011; Macnamara & Roberts 2010; Luna-Cardozo et al. 2012, and references therein).

Complementing the fact that the detection of MHD waves is gaining sufficient importance in the development of refined MHD seismology techniques to understand the properties of solar corona, it is also worth stating that there have been several attempts to detect various MHD waves in the stellar coronae of

Sun-like stars (e.g., Stepanov et al. 2001; Mathioudakis et al. 2003, 2006; Mitra-Kraev et al. 2005; Pandey & Srivastava 2009; Anfinogentov et al. 2013). The origins of such oscillations are still under debate, however, it has recently been proposed that they can be produced by several mechanisms during flaring activities in the magnetized coronae of Sun-like stars (e.g., Nakariakov & Melnikov 2009, and references therein). The widely accepted scenario behind the evolution of such quasi-periodic oscillations is the excitation of MHD wave modes in stellar coronal structures. In recent work, slow-mode oscillations were reported first by Mitra-Kraev et al. (2005) in the flaring loop of AT Mic, while magnetoacoustic kink waves were reported by Pandey & Srivastava (2009) in the corona of ξ -Boo. Mathioudakis et al. (2006) reported on the observational scenario of very high frequency oscillations in the atmosphere of the active star EQ Peg B, which may be excited either by fast MHD waves or due to repetitive magnetic reconnection. Recently, Anfinogentov et al. (2013) found evidence of various types of MHD oscillations in the dMe star YZ CMi. However, most of the attempts in previous works were related to the detection of single MHD mode oscillations in stellar coronae and their loops. To the best of our knowledge, there have been no extensive efforts to detect multiple MHD modes and thus the related basic seismology of stellar coronae.

In this Letter, we first detect the first two harmonics of slow magnetoacoustic oscillations in the corona of the dMe star Proxima Centauri using observations carried out by *XMM-Newton*. The Letter is organized as follows: in Section 2, we briefly present the observations and adopted loop parameters. We describe the detection of MHD modes in Section 3. In Section 4, we explain the MHD seismology of the corona of Proxima Centauri. The discussion and conclusions are found in Section 5.

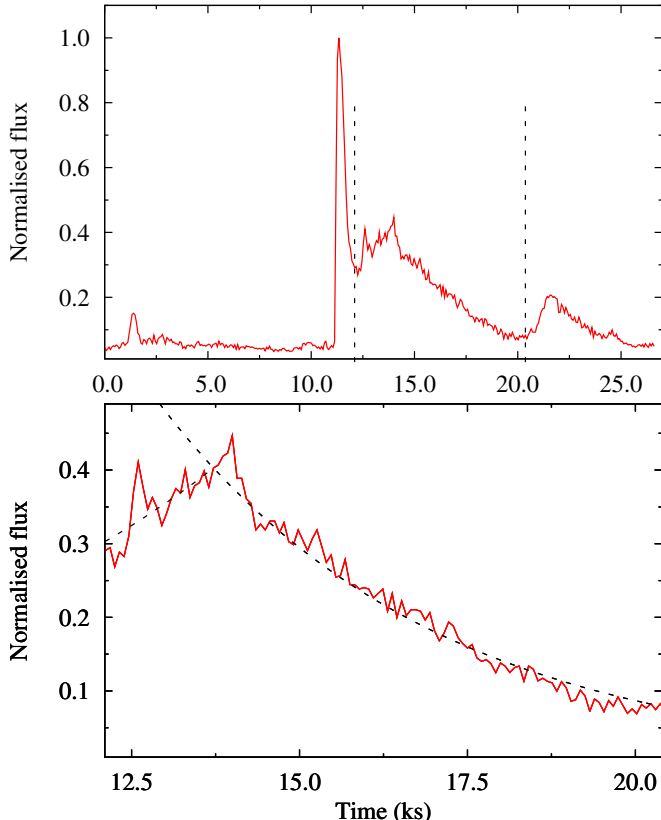


Figure 1. Top panel: *XMM-Newton* light curve of Proxima Centauri in the 0.3–10 keV energy band with a binning time of 70 s. The detected oscillations are localized during 12–21 ks as shown between the two vertical dashed lines. Bottom panel: the best-fit exponential function along with the light curve under the dashed line as shown in the top panel. The best-fit exponentials were used to remove long-term trends associated with flare background effects.

(A color version of this figure is available in the online journal.)

2. OBSERVATIONS

We choose a flaring epoch in the corona of Proxima Centauri observed with the *XMM-Newton* satellite using the European Photon Imaging Camera (EPIC) detector on 2009 March 13–14 (Observation ID: 0551120401). Details of the observations and data reduction are given in Fuhrmeister et al. (2011). The top panel of Figure 1 shows the light curve of a flaring epoch of Proxima Centauri in the 0.3–10.0 keV energy band. The flare starts at 06:00 UT, peaks at 06:45 UT, and shows a long decay phase up to 09:00 UT on 2009 March 14. The region between the two dashed vertical lines is the region of interest where we searched for localized MHD oscillation candidates. The bottom panel of Figure 1 shows this localized temporal span of the light curve during 12–21 ks, in which best-fit exponential functions of the form $I = I_0 e^{\pm(t-t_0)/\tau_d}$ are fitted to remove long-term background flare variations. Using spectral modeling, the flare peak temperature was derived as $33^{+7.73}_{-11.93}$ MK. However, the average temperature during the post-flare phase (i.e., a flare duration of between 12–21 ks) was derived as 7.2 ± 0.6 MK (see Table 3 of Fuhrmeister et al. 2011).

2.1. Estimation of Loop Length

Using the time-dependent hydrodynamic loop model of Reale et al. (1997), Fuhrmeister et al. (2011) derived a loop half-length of $8.55^{+3.81}_{-2.86} \times 10^9$ cm. This method includes both plasma cooling and the effect of heating during flare decay,

Table 1
The Summary of Detected Periodicities using Wavelet Analysis

Binning Time (s)	Cycles	Periods (s)	Probability (%)
50	>3	1274 and 694	>99
60	>3	1286 and 701	>99
70	>3	1261 and 687	>99
90	>3	1250 and 682	>97

but sometimes overestimates the loop length (Reale 2007). If we assume that the flare emission originated from an ensemble of coronal loops with a uniform cross section and a roughly semicircular midplane shape, then we can express the observed volume emission measure (VEM) in terms of the loop length (L), density (n_e), number of loops (N), and aspect ratio (α). Following Huenemoerder et al. (2001), the loop length is derived as $L = \pi^{-1/3} \alpha^{-2/3} N^{-2/3} \text{VEM}^{1/3} n_e^{-2/3}$. Using a peak emission measure for the flare of $9.62 \pm 1.88 \times 10^{50}$ cm³ and a density of $6.9 \pm 2.6 \times 10^{10}$ cm⁻³ (Fuhrmeister et al. 2011), and assuming 100 flaring loops with an aspect ratio of 0.1, the loop length was calculated to be $4.0 \pm 1.0 \times 10^9$ cm. Using the statistical loop length and peak temperature relation, $L = 10^{9.4} T_p^{0.91}$, which leads to the theoretically predicted scaling law of $\text{EM}_P \propto T_p^{4.3}$ and further explains the observed correlation of $\text{EM}_P \propto T_p^{4.7 \pm 0.4}$ for both solar and stellar flares (Aschwanden et al. 2008), the loop length is calculated to be $7.5^{+1.4}_{-2.2} \times 10^9$ cm. The loop lengths derived from the two methods above are consistent with each other. However, these loop lengths are smaller than that derived from a single-loop hydrodynamic model. Our derived loop length using the multi-loop model is similar to those derived for other flaring dwarfs (Pandey & Singh 2008), therefore for further analyses we have used a loop length of 7.5×10^9 cm.

3. DETECTION OF HARMONIC PERIODS IN THE CORONA OF PROXIMA CENTAURI

We used the wavelet analysis IDL code “Randomlet” which performs randomization tests (O’Shea et al. 2001) along with the standard wavelet analysis (Torrence & Compo 1998) to examine the statistically significant real periodicities in the time series data and to compute the associated powers. We used the flare light curve in the 0.3–10 keV energy band and varied the time bin size from 50–90 s. We clearly notice a consistent and localized oscillatory pattern in the post-flare phase of the emission (see Figure 1). We did not choose the lower binning as we were not interested in the very high frequency oscillations of stellar loops. Using the standard wavelet tool as discussed above, we derived the power spectra for each of these light curves during the post-flare phase between 12–20 ks. We detected almost similar harmonic periods in each binning of the data (see Table 1). Here we present one example of the detected harmonic periods in Figure 2, related to the 70 s binned data.

Depicted in Figure 2 is the result from the wavelet analysis, in which the top panel displays the de-trended light curve of the 70 s binned data during the post-flare phase heightened emissions (see top and bottom panels of Figure 1). In the left-hand middle panel of Figure 2, we plot the intensity wavelet that shows the bursty and localized nature of the oscillations and related powers. These oscillatory periods of 1261 and 687 s were sustained for 90 and 50 minutes with >3 cycles, respectively. The right-hand middle panel in Figure 2 shows the global power spectrum with a significant periodicity of

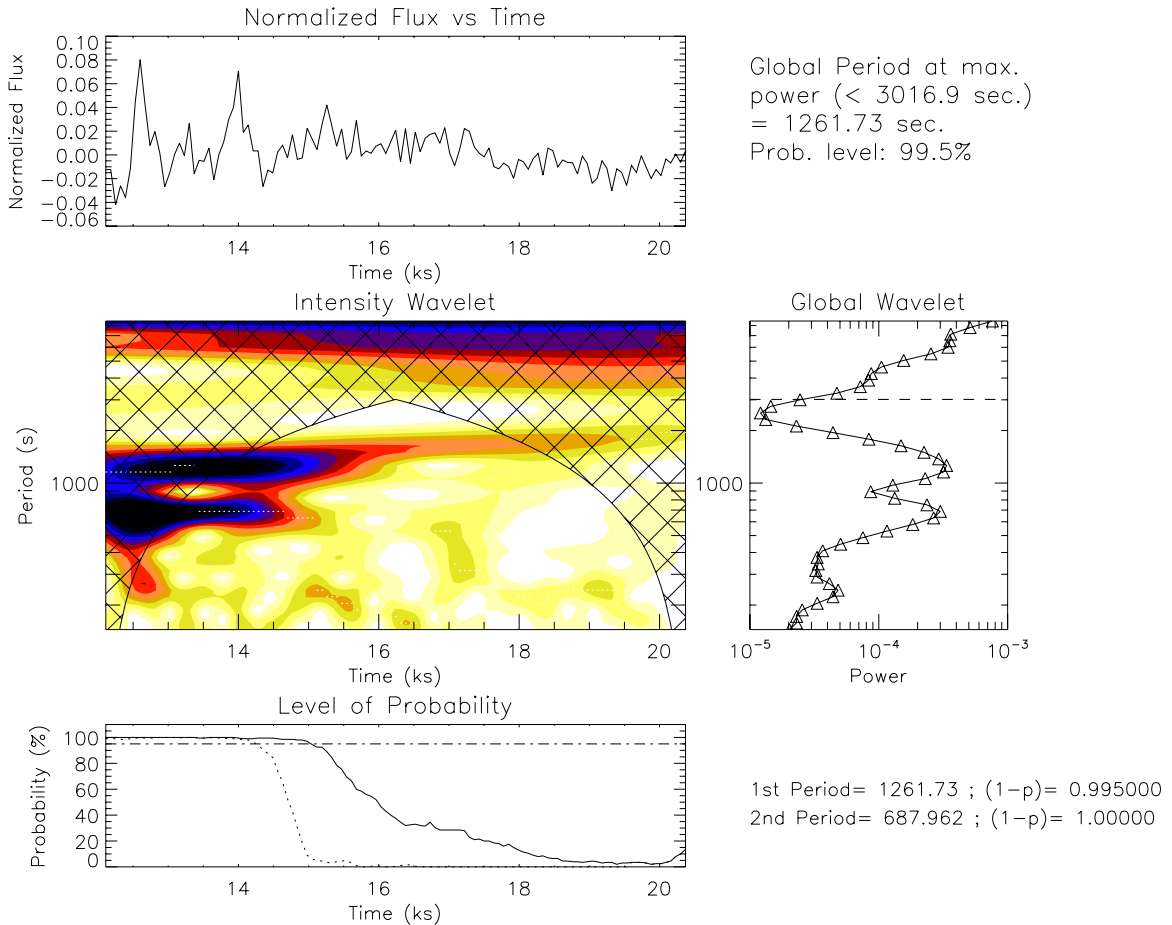


Figure 2. Wavelet result. The top panel shows the detrended light curve removed from the flare background; the left-hand middle panel shows the intensity wavelet; the right-hand middle panel shows the global power spectrum with a significant periodicity of 1261 s with a probability of 99.5%. The other period and related power are concentrated around ~ 687 s in the intensity wavelet. The bottom panel shows the probability variation of the two detected periodicities.

(A color version of this figure is available in the online journal.)

1261 s with a probability greater than 99%. We notice that the other bursty power lies at 687 s in the intensity wavelet and corresponding global power peak is also present. The bottom panel displays the temporal variation of the probabilities related to the detected multiple periods that lie in the localized time-span in the intensity wavelet. The other larger periods (> 3000 s) may persist in the untrended light curve, however, we searched for the periods that are naturally excited and associated with the possible MHD modes excited in flaring stellar loops with certain morphological and plasma properties. Therefore, the periods of interest, which are most likely associated with the MHD activity of the loops, can only be detected after pre-whitening of these long-term variations (O’Shea et al. 2007; Anfinogentov et al. 2013). The wavelet results are consistent with the Lomb–Scargle periodogram analyses of the same light curve (Scargle 1982). In Figure 3, we show the detection of almost similar periodicities near ~ 1261 s and ~ 687 s, which are above the 1σ level. A higher period of 8000 s is also seen in the power spectra, which is equivalent to the total data length. However, such long periods may not be real and may lie outside the cone-of-influence of the wavelet. Significant detections of naturally evolved periods in 50–90 s time-binned light curves are summarized in Table 1. It should also be noted that the EPIC-MOS light curves of these different binnings also exhibit similar periodicities.

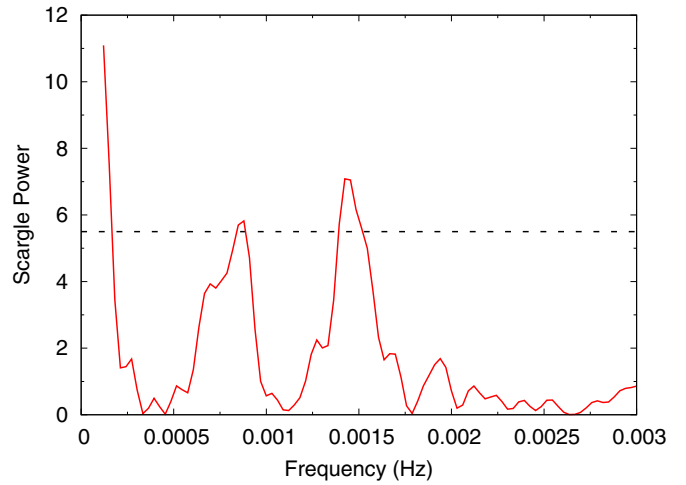


Figure 3. Power spectra of detrended light curve as shown in the top panel of Figure 2. The horizontal line is the 1σ level significance. The detection of the edged and unrealistic period of 8000 s is also evident in the periodogram that suppresses the power and significance of two naturally evolved periods.

(A color version of this figure is available in the online journal.)

4. MHD SEISMOLOGY IN THE LOCALIZED CORONA OF PROXIMA CENTAURI

The observed harmonic periods (1261 and 687 s) may be due to the impulsive generation of slow MHD oscillations as a consequence of flare energy release. The harmonic period of 687 s is only present during the first 3 ks (see Figure 2), which is likely to be an overtone that results from the initial spontaneous excitation of the slow-mode wave, but damped out more quickly than the fundamental period of 1261 s. The observed oscillations may be excited in this loop due to the impulsive flare energy release and heating of the loops (Nakariakov et al. 2004; Mendoza-Briceño & Erdélyi 2006; Selwa et al. 2007). Using the loop length of 7.5×10^9 cm, the phase speed of the fundamental mode MHD oscillations for a period of 1261 s is estimated to be 119 km s^{-1} , which is sub-sonic in nature compared to the local sound speed (394 km s^{-1}) in the loop at an average temperature of 7.2 MK during the post-flare phase. However, the peak flare temperature of 33 MK corresponds to the local sound speed of 850 km s^{-1} . This impulsive heating may initially trigger the slow oscillations, however, they span the localized decay phase where the loop quickly cools down and is maintained at an average temperature of 7.2 MK. Therefore, the detected periodicities could be due to the first two harmonics of the slow acoustic MHD oscillations in the coronal loops of Proxima Centauri. In the case of slow magnetoacoustic oscillations, the density of the loop is perturbed due to the spatial redistribution of the plasma along the background magnetic field, i.e., the field-aligned movement of the plasma from one footpoint to the other in the case of the fundamental mode, and from both the footpoint to the apex in the case of its first overtone (Kim et al. 2012). Therefore, these MHD modes significantly modulate the emissions of the plasma. As the observed energy release is very powerful, the solar analogy suggests that it may also be a two-ribbon flare and the slow-mode oscillations can be excited in a system of plasma arcades (Nakariakov & Zimovets 2011; Gruszecki & Nakariakov 2011). However, the arcade model, as opposed to the loop model, does not change the above-mentioned conclusions as the observations do not have spatial resolution.

Such types of oscillations have already been detected in hot and flaring loops (Ofman & Wang 2002; Nakariakov et al. 2004; Kim et al. 2012), as well as in comparatively cooler non-flaring loops (Srivastava & Dwivedi 2010) in the solar corona. Such oscillations show the strong nature of damping, which is most likely due to thermal conduction (Ofman & Wang 2002). In the case presented here, the fundamental mode of the oscillations shows strong damping. In the case of the fundamental mode wave period, the peak intensity decays up to its $1/e$ value in ~ 50 minutes, which is the damping time of such oscillations.

Figure 4 shows the variation of the exponentially decaying harmonic function along with the detrended light curve. The function is described as

$$F(t) = \sum_{i=1}^2 A_i \cos\left(\frac{2\pi}{P_i} \cdot t + \phi_i\right) e^{-\frac{\delta}{P_i} \cdot t}, \quad (1)$$

where A_i and ϕ_i are the amplitudes and phases corresponding to the oscillatory period, P_i (1261 s and 687 s), respectively, and δ is the damping factor. The best fit of the function (see Figure 4) gives $\delta = 0.45$, which indicates a damping time of 47 minutes. It is well-fitted to the noisy light curve that was used in the detection of these two periodicities (see Figures 3 and 4). The

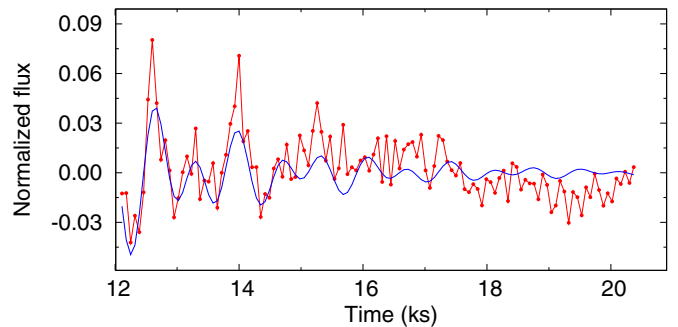


Figure 4. Detrended light curve of the post-flare phase along with the best-fit exponentially decaying harmonic function as given by Equation (1). (A color version of this figure is available in the online journal.)

synthesized curve shows a damping period of 47 minutes, which is similar to the observed damping time of 50 minutes when the initial amplitude of the oscillations decays to its $1/e$ value in the observational baseline (see top panel of Figure 2). The observed damping time is almost in agreement with the scaling laws between the observed wave period and decay time of such oscillations as reported in a variety of hot loops in solar corona as observed by the Solar Ultraviolet Measurement of Emitted Radiation (SUMER) onboard *SOHO* (Ofman & Wang 2002). Therefore, we may also conclude that the strong damping of such oscillations is due to the effect of thermal conduction in the loops of Proxima Centauri.

We use the solar analogy to derive the plasma conditions of the corona of the spatially unresolved low mass flaring star Proxima Centauri (e.g., McEwan et al. 2006; Srivastava & Dwivedi 2010; Macnamara & Roberts 2010; Luna-Cardozo et al. 2012, and references therein). The period ratio P_1/P_2 is derived as 1.83. This period ratio of less than 2.0 is most likely due to the longitudinal density stratification of the stellar loops of the star in which such oscillations are excited. The effect of density stratification on the lowering of the period ratio of the first two harmonics of slow acoustic oscillations has only been studied in the case of solar corona loops, which provides the most likely longitudinal density structuring of such loops (e.g., McEwan et al. 2006; Srivastava & Dwivedi 2010; Macnamara & Roberts 2010; Luna-Cardozo et al. 2012, and references therein). It should be noted that the lowering in the period ratio of the first two harmonics of slow magnetoacoustic waves attributes only to the density stratification. However, in the case of kink waves, the period ratio can either be less than or greater than 2, implying the density stratification and magnetic field divergence of the magnetic fluxtubes, respectively (Andries et al. 2009).

The observations presented here provide the first clues regarding longitudinal density structuring in stellar flaring loops. Therefore, such density or gravitational stratification should be considered in future modeling of stellar loops. Using Equation (24) of McEwan et al. (2006), a half loop length of 3.75×10^9 cm, and a period ratio ($P_1/2P_2$) of 0.917, the density scale height of the stellar loop system is estimated as ~ 23 Mm. The density scale height is well below the hydrostatic scale height of such loops, assuming a typical coronal temperature of a few MK in Proxima Centauri during the non-flaring state. This indicates the existence of non-equilibrium conditions, e.g., flows and mass structuring, which is very obvious in the dynamical coronae of such stars. For example, hot gas motions have been seen in the optical and ultraviolet spectra of

the flaring M dwarfs DENIS 104814.7-395606.1 and CN Leo (Fuhrmeister & Schmitt 2004; Fuhrmeister et al. 2004). However, such physical scenarios are not well established in the case of stellar coronae (e.g., Güdel & Nazé 2010).

5. SUMMARY AND DISCUSSION

Heating due to flaring activity either near the apex or near the footpoints of a loop can generate the various modes of slow acoustic oscillations in magnetic loops (Nakariakov et al. 2004), or in loop–arcade systems in the flaring region (Nakariakov & Zimovets 2011; Gruszecki & Nakariakov 2011). Random heating near the footpoint of these loops may also cause the excitation of the slow acoustic oscillations (Mendoza-Briceño & Erdélyi 2006). Taroyan & Bradshaw (2008) have shown that the various harmonics of slow acoustic oscillations may be present in coronal loops maintained at a variety of temperatures, i.e., in hot as well as cool loops. More recently, harmonic periods have been observed in cool non-flaring loops as observed by Srivastava & Dwivedi (2010). Previously, the slow acoustic oscillations had only been discovered in hot SUMER loops (Ofman & Wang 2002). However, the excitation conditions, and typically the observations of such significant MHD modes, in the solar atmosphere are still under debate.

We present the first observational evidence of harmonic periods (1261 and 687) of slow acoustic oscillations in the flaring coronal loop system of Proxima Centauri. The observed shorter periodicity (687 s) may be connected with the anharmonicity of the main periodicity (1261 s) and therefore may not be associated with another mode of oscillations. The appearance of such oscillations are bursty and temporally localized in the post-flare phase which may be generated due to spontaneous heating of the stellar loops of Proxima Centauri after the flare energy release. The fundamental mode oscillations show a strong decaying nature similar to the slow acoustic oscillations observed in the solar corona. Therefore, it may also be most likely caused by thermal conduction (Ofman & Wang 2002). One additional interesting property is evident in the form of the period shift of the fundamental mode slow acoustic oscillations. The period is shifted toward higher values (see the intensity wavelet of Figure 2). This indicates a change in the local sound speed, which is the upper bound of the phase speed of the detected slow magnetoacoustic oscillations in an ideal plasma, as $P(T(t)) \propto 1/C_s(T(t))$ (Aschwanden 2004). This means that the local phase speed of slow acoustic oscillations will decrease with the shift of the period toward higher values up to the time domain of 90 minutes. This indicates that the local ambient temperature of the loops may be decreased due to radiative cooling and can cause dissipation of these oscillations (e.g., Aschwanden 2004). However, radiative cooling may not play an important role in dissipating the fast kink or sausage modes as the typical timescale of the radiative cooling (1 hr) in solar-type loops may be higher compared to the damping time of these modes as theorized in various reports (Morton & Erdélyi 2009; Ruderman 2011).

This may be the most plausible non-ideal effect that can also cause damping of such oscillations. The period ratio P_1/P_2 is found to be 1.83, which may be the most likely signature of density stratification in these stellar loops. The estimated density scale height is ~ 23 Mm, which is well below the hydrostatic scale height of such loops. This indicates the presence of non-equilibrium conditions in its corona, i.e., mass structuring as well as flows.

We thank the reviewer for his valuable suggestions that improved the manuscript considerably, and Professor Mihalis Mathioudakis for reading the manuscript and providing useful suggestions. This work uses data obtained by *XMM-Newton*, an ESA science mission with instruments and contributions directly funded by ESA Member States and the USA (NASA). A.K.S. thanks Shobhna Srivastava for her support and encouragement.

REFERENCES

- Andries, J., van Doorsselaere, T., Roberts, B., et al. 2009, SSRv, **149**, 3
 Anfinogentov, S., Nakariakov, V. M., Mathioudakis, M., Van Doorsselaere, T., & Kowalski, A. F. 2013, ApJ, **773**, 156
 Aschwanden, M. J. 2004, Physics of Solar Corona (Berlin: Springer)
 Aschwanden, M. J., Fletcher, L., Schrijver, C. J., & Alexander, D. 1999, ApJ, **520**, 880
 Aschwanden, M. J., & Schrijver, C. J. 2011, ApJ, **736**, 102
 Aschwanden, M. J., Stern, R. A., & Güdel, M. 2008, ApJ, **672**, 659
 Cirtain, J. W., Golub, L., Lundquist, L., et al. 2007, Sci, **318**, 1580
 De Pontieu, B., McIntosh, S. W., Carlsson, M., et al. 2007, Sci, **318**, 1574
 Fuhrmeister, B., Lalitha, S., Poppenhaeger, K., et al. 2011, A&A, **534**, A133
 Fuhrmeister, B., & Schmitt, J. H. M. M. 2004, A&A, **420**, 1079
 Fuhrmeister, B., Schmitt, J. H. M. M., & Wichmann, R. 2004, A&A, **417**, 701
 Gruszecki, M., & Nakariakov, V. M. 2011, A&A, **536**, A68
 Güdel, M., & Nazé, Y. 2010, SSRv, **157**, 211
 Huenemoerder, D. P., Canizares, C. R., & Schulz, N. S. 2001, ApJ, **559**, 1135
 Jess, D. B., Mathioudakis, M., Erdélyi, R., et al. 2009, Sci, **323**, 1582
 Kim, S., Nakariakov, V. M., & Shibasaki, K. 2012, ApJL, **756**, L36
 Luna-Cardozo, M., Verth, G., & Erdélyi, R. 2012, ApJ, **748**, 110
 Macnamara, C. K., & Roberts, B. 2010, A&A, **515**, A41
 Mathioudakis, M., Bloomfield, D. S., Jess, D. B., Dhillon, V. S., & Marsh, T. R. 2006, A&A, **456**, 323
 Mathioudakis, M., Jess, D. B., & Erdélyi, R. 2013, SSRv, **175**, 1
 Mathioudakis, M., Seiradakis, J. H., Williams, D. R., et al. 2003, A&A, **403**, 1101
 McEwan, M. P., Díaz, A. J., & Roberts, B. 2008, A&A, **481**, 819
 McEwan, M. P., Donnelly, G. R., Díaz, A. J., & Roberts, B. 2006, A&A, **460**, 893
 McIntosh, S. W., de Pontieu, B., Carlsson, M., et al. 2011, Natur, **475**, 477
 Mendoza-Briceño, C. A., & Erdélyi, R. 2006, ApJ, **648**, 722
 Mitra-Kraev, U., Harra, L. K., Williams, D. R., & Kraev, E. 2005, A&A, **436**, 1041
 Morton, R. J., & Erdélyi, R. 2009, ApJ, **707**, 750
 Nakariakov, V. M., & Melnikov, V. F. 2009, SSRv, **149**, 119
 Nakariakov, V. M., Ofman, L., Deluca, E. E., Roberts, B., & Davila, J. M. 1999, Sci, **285**, 862
 Nakariakov, V. M., Tsiklauri, D., Kelly, A., Arber, T. D., & Aschwanden, M. J. 2004, A&A, **414**, L25
 Nakariakov, V. M., & Verwichte, E. 2005, LRSP, **2**, 3
 Nakariakov, V. M., & Zimovets, I. V. 2011, ApJL, **730**, L27
 Ofman, L., & Wang, T. 2002, ApJL, **580**, L85
 O’Shea, E., Banerjee, D., Doyle, J. G., Fleck, B., & Murtagh, F. 2001, A&A, **368**, 1095
 O’Shea, E., Srivastava, A. K., Doyle, J. G., & Banerjee, D. 2007, A&A, **473**, L13
 Pandey, J. C., & Singh, K. P. 2008, MNRAS, **387**, 1627
 Pandey, J. C., & Srivastava, A. K. 2009, ApJL, **697**, L153
 Reale, F. 2007, A&A, **471**, 271
 Reale, F., Betta, R., Peres, G., Serio, S., & McTiernan, J. 1997, A&A, **325**, 782
 Ruderman, M. S. 2011, SoPh, **271**, 41
 Scargle, J. D. 1982, ApJ, **263**, 835
 Selwa, M., Ofman, L., & Murawski, K. 2007, ApJL, **668**, L83
 Srivastava, A. K., & Dwivedi, B. N. 2010, NewA, **15**, 8
 Srivastava, A. K., Zaqrashvili, T. V., Uddin, W., Dwivedi, B. N., & Kumar, P. 2008, MNRAS, **388**, 1899
 Stepanov, A. V., Kliem, B., Zaitsev, V. V., et al. 2001, A&A, **374**, 1072
 Taroyan, Y., & Bradshaw, S. 2008, A&A, **481**, 247
 Torrence, C., & Compo, G. P. 1998, BAMS, **79**, 61
 Verth, G., & Erdélyi, R. 2008, A&A, **486**, 1015
 Verwichte, E., Aschwanden, M. J., Van Doorsselaere, T., Foullon, C., & Nakariakov, V. M. 2009, ApJ, **698**, 397
 Wang, T. 2011, SSRv, **158**, 397